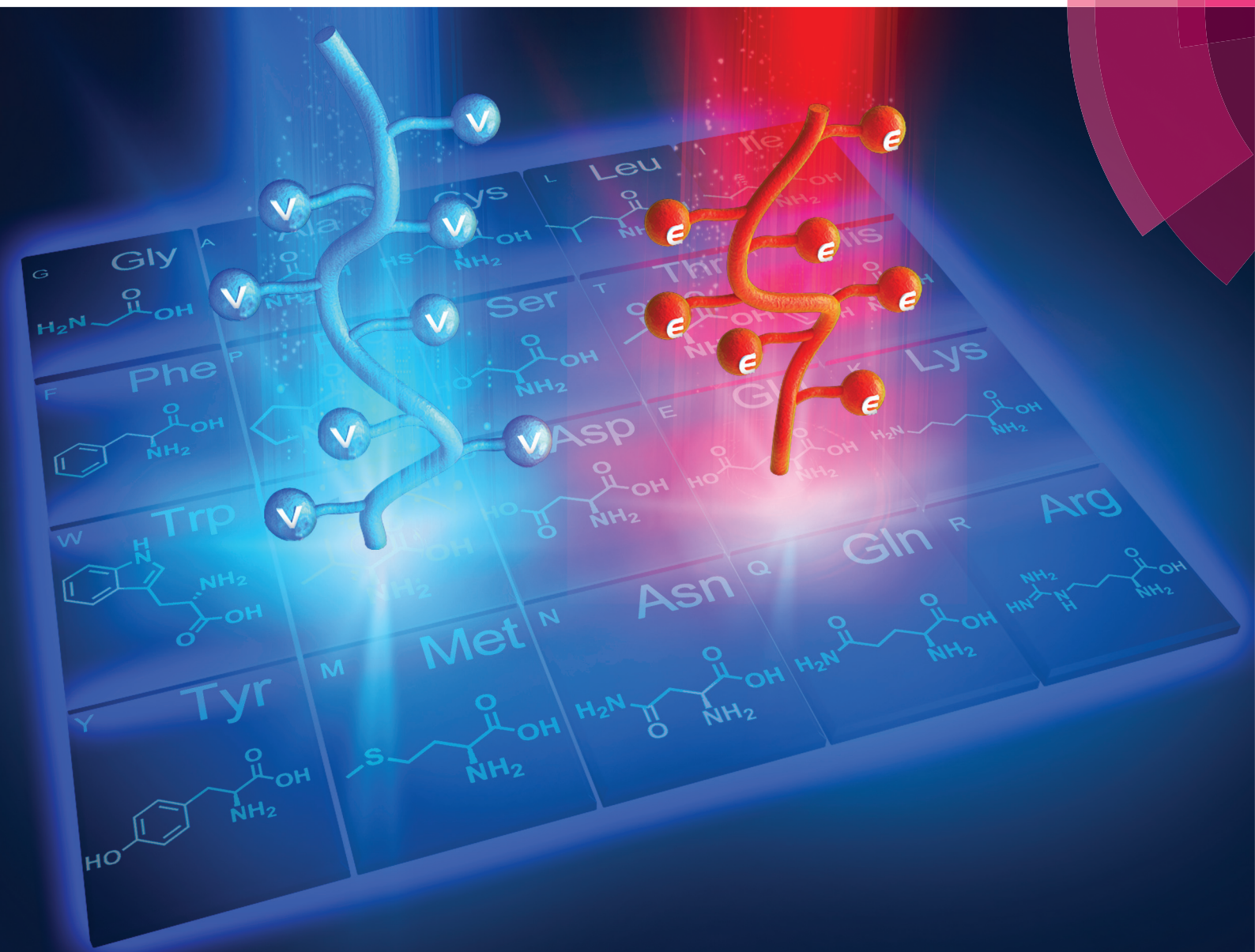


Polymer Chemistry

rsc.li/polymers



ISSN 1759-9962



ROYAL SOCIETY
OF CHEMISTRY

PAPER

Xing Wang, Jiangtao Xu *et al.*

Precise synthesis of poly(*N*-acryloyl amino acid) through photoinduced living polymerization



Cite this: *Polym. Chem.*, 2018, **9**, 2733

Precise synthesis of poly(*N*-acryloyl amino acid) through photoinduced living polymerization†

Guofeng Li,^{a,b} Wenli Feng,^a Nathaniel Corrigan,^b Cyrille Boyer,^b Xing Wang^b and Jiangtao Xu^b

Amino acid-based polymers possess exceptional physical structures, chemical properties, and biocompatibility and have shown great potential in applications, including drug delivery, chiral recognition, and sensor materials, among others. The precise synthesis of amino acid-based polymers with defined chemical structure and functionality facilitates the exploration of prospective properties and therefore potential practical applications. Controlled/"living" radical polymerization techniques are powerful tools for the synthesis of amino acid-based polymers due to their tolerance toward functional groups and versatility of polymerisable monomer families. In this work, we used photoinduced electron/energy transfer-reversible addition–fragmentation chain transfer (PET-RAFT) polymerization to polymerize various *N*-acryloyl amino acid monomers with diverse chirality and functionality to prepare a library of amino acid-based polymers with controlled molecular weights and narrow molecular weight distributions ($M_w/M_n < 1.20$) under mild conditions. Different solvents, RAFT agents and photocatalysts have been investigated to show the robustness and versatility of this process. Amino acid monomers with unprotected di-carboxylic acid moieties were directly polymerized in methanol to provide a facile approach to prepare various well-defined homo- and di-block amino acid-based polymers.

Received 5th March 2018,
Accepted 18th April 2018

DOI: 10.1039/c8py00366a
rsc.li/polymers

Introduction

Amino acids are the basic building units of proteins, and dictate protein chemical structures and biological functions through their remarkably diverse physical and chemical properties, including hydrophobicity, hydrophilicity, net charge, stereoregularity and functionality, *etc.* Therefore, the introduction of amino acid units into synthetic polymers endows these materials with outstanding biocompatibility, biodegradability and stimuli-responsive properties, as well as the ability to form highly ordered hierarchical structures.^{1–3} As a result, amino acid containing synthetic polymers are important candidates for applications in various areas,^{4,5} such as drug delivery,^{6–12} surface antifouling,^{13,14} chiral recognition,^{15,16} metal ion absorption,¹⁷ and polyelectrolytes.^{18–21}

The incorporation of amino acid moieties in polymers is historically performed using two distinct strategies; (1) synthesis of poly(amino acid)s (polypeptide or polypeptoid) as protein biomimics through polycondensation of various amino acids, or ring-opening polymerization of *N*-carboxyanhydrides,^{5,22–24} or (2) synthesis of polymers bearing amino acid side chains through polymerization of the corresponding amino acid containing monomers, or post-modification of reactive polymer functional groups with amino acids functionalities (carboxylic acid, amine, thiol and hydroxyl, *etc.*)^{25–30} The first strategy has focused on polymers comprising amino acid moieties in the main chain, which are structurally analogous to naturally occurring polypeptides. While this strategy produces protein mimics that are structurally equivalent to natural proteins, the production methods are complex and tedious. The synthetic polymers produced using the second strategy may not self-assemble into β -sheets or α -helices, but are still of significant interest for their capacity to respond to external stimuli such as pH and temperature, to bind to metal ions, and to modulate cell–interface interactions. From a synthetic standpoint, the second strategy is advantageous, as various state-of-the-art polymerization techniques can be employed. These techniques have intrinsically broad monomer diversity, less stringent reaction conditions, and as such, present greater industrial viability for manufacturing.

^aBeijing Advanced Innovation Center for Soft Matter Science and Engineering, Beijing Laboratory of Biomedical Materials, Beijing University of Chemical Technology, Beijing 100029, P. R. China. E-mail: wangxing@mail.buct.edu.cn

^bCentre for Advanced Macromolecular Design and Australian Centre for NanoMedicine, School of Chemical Engineering, University of New South Wales, Sydney 2052, Australia. E-mail: j.xu@unsw.edu.au

†Electronic supplementary information (ESI) available: Experimental details, NMR spectra, UV-vis spectra and GPC traces (Fig. S1–S29). See DOI: 10.1039/c8py00366a

In the past two decades, controlled/"living" radical polymerization (CRP) techniques, including nitroxide-mediated polymerization (NMP), atom transfer radical polymerization (ATRP), and reversible addition-fragmentation chain transfer (RAFT) polymerization, have been successfully employed for precise synthesis of polymers bearing amino acid substituents.^{2,31–35} A significant benefit of CRP techniques, particularly RAFT, is the tolerance over monomer functionality (free primary and secondary amines are challenging for RAFT), thus readily allowing the controlled polymerization of functional amino acids.^{31,36,37} Endo and coworkers first reported the polymerization of methyl ester acrylamide phenylalanine *via* the RAFT technique in 2005.³⁸ In the next year, they extended their work to polymerize unprotected acid derivatives of phenylalanine.³⁹ More recently, De and coworkers developed a series of amino acid-based polymers through RAFT polymerization of C-terminus modified vinyl monomers, and studied the self-contained behavior of these polymers.^{2,27,40,41} McCormick and coworkers have also reported that aqueous RAFT polymerization can be utilized to synthesize well-controlled homo- and block copolymers based on the *N*-acryloyl-alanine monomers under optimized conditions.^{42,43} Although a great number of efforts have been dedicated to synthesizing various polymer structures, the synthetic protocols are still complicated and need to be applied on a case by case basis. The systematic studies on the polymerization of different types of amino acid-based vinyl monomers are still limited, and a universal methodology is quite desirable. Therefore, this contribution is dedicated to the synthesis of *N*-acryloyl amino acid monomers with different amino acid substituents, and subsequently, preparation of the corresponding amino acid-based polymers with well-defined chemical structures, through a robust and versatile living radical polymerization technique.

Photoinduced electron/energy transfer-reversible addition-fragmentation chain transfer (PET-RAFT) polymerization is a highly efficient photoinduced living radical polymerization technique.⁴⁴ The unique mechanism of this technique consists of two processes, photoinduced electron/energy transfer (PET) and the RAFT process. In the PET-RAFT process, a visible light photoredox catalyst initially absorbs light to produce an excited state (triplet) photocatalyst. The excited triplet species then interacts with thiocarbonylthio compounds (RAFT agents) to produce a radical that initiates the RAFT process.^{44,45} This novel polymerization technique presents great advantages in living polymerization and macromolecular design. The PET-RAFT process also possesses selective photoactivation properties which have been exploited for polymerization⁴⁶ and the synthesis of sequence-defined oligomers through a successive single unit monomer insertion (SUMI) approach.⁴⁷ More importantly, the PET-RAFT technique is strongly tolerant toward molecular oxygen^{48,49} and various functional monomers;⁴⁴ it can be performed in the presence of air or under mild reaction conditions as well as in ultralow volume setups.^{50–53}

In this work, the PET-RAFT technique is employed using various RAFT agents to polymerize a range of *N*-acryloyl amino

acid monomers with diverse chirality (*D*- and *L*-) and different functionalities, including ester, hydroxyl, mono- and di-carboxylic acid moieties. The corresponding homopolymers and diblock copolymers will be prepared and assessed on molecular weights and molecular weight distributions. This comprehensive study will create a library of amino acid-based polymers derived from *N*-acryloyl amino acid monomers. Importantly, we have addressed the challenge of well-controlled polymerization of unprotected di-carboxylic acid monomers under mild reaction conditions, which has scarcely been achieved in previous reports.

Experimental section

Materials

Valine methyl ester (99%), *L*(*D*)-valine (99%), *L*-serine (99%), *D*-phenylalanine (99%), *L*(*D*)-aspartic acid (99%), *L*-glutamic acid (99%), *L*-di-*tert*-butyl 2-aminopentanedioate hydrochloride (97%), acryloyl chloride (97%), 2',4',5',7'-tetrabromofluorescein (Eosin Y, 99%), 5,10,15,20-tetraphenyl-21*H*,23*H*-porphine zinc (ZnTPP, 98%), tris[2-phenylpyridinato-C²,N]iridium(III) (Ir(ppy)₃, 99%), 2-(dodecylthiocarbonothioylthio)-2-methylpropionic acid (DDMAT, 98%), 2-cyano-2-propyl dodecyl trithiocarbonate (CPTC, 97%), and trimethylsilyldiazomethane (TMSCHN₂, *ca.* 10% in hexane, 0.6 mol L⁻¹) were all purchased from Sigma-Aldrich and used as received. Diethyl ether, dichloromethane (DCM), tetrahydrofuran (THF), *N,N*-dimethylformamide (DMF), dimethyl sulfoxide (DMSO), methanol (MeOH), 1,4-dioxane (Diox), acetonitrile (MeCN), toluene, HCl and NaOH were purchased from Ajax Chemical and used as received. 2-(Dodecylthiocarbonothioylthio) propionic acid (DTPA) was purchased from Boron Molecular and used as received. 2-(1-Carboxy-1-methylethylsulfanylthiocarbonylsulfanyl)-2-methylpropionic acid (CMP) was synthesized according to the literature.⁵⁴

Instrumentation

Gel permeation chromatography (GPC) was used to characterize synthesized polymers with *N,N*-dimethylacetamide (DMAc) as the eluent. The GPC instrument consists of Shimadzu modular system with an autoinjector, a Phenomenex 5.0 μM bead sizeguard column (50 × 7.5 mm) followed by four Phenomenex 5.0 μM bead size columns (105, 104, 103 and 102 Å), a differential refractive index detector, and a UV detector (λ = 305 nm). The DMAc system was calibrated based on low dispersity polymethyl methacrylate (PMMA) standards with molecular weights of 200 to 10⁶ g mol⁻¹. The measurements were performed at 50 °C, at a flow rate of 1 mL min⁻¹. Polymers with free carboxylic acid functionality were methylated by TMSCHN₂ prior to GPC measurement.⁵⁵

Nuclear magnetic resonance (NMR) spectroscopy was carried out on Bruker Avance III with SampleXpress operating at 400 MHz for ¹H and 100 MHz for ¹³C NMR using DMSO-*d*₆ and CDCl₃ as solvents. Tetramethylsilane (TMS) was used as a

reference. The data obtained was reported as chemical shift (δ) measured in ppm downfield from TMS.

UV-vis spectroscopy spectra were recorded using a CARY 300 spectrophotometer (Varian).

On-line Fourier Transform Near-Infrared (FTNIR) spectroscopy was used to measure the monomer conversions by following the decrease of the vinylic C–H stretching overtone of the monomer at $\sim 6200\text{ cm}^{-1}$. A Bruker IFS 66/S Fourier transform spectrometer equipped with a tungsten halogen lamp, a CaF₂ beam splitter and liquid nitrogen cooled InSb detector was used. The sample was placed in a FTNIR quartz cuvette (1 cm \times 2 mm) and polymerized under blue LED light irradiation ($\lambda_{\text{max}} = 460\text{ nm}$). Every 10 min, the sample was put into holder manually and each spectrum in the spectral region of 7000–5000 cm^{-1} was constructed from 32 scans with a resolution of 4 cm^{-1} . The total collection time per spectrum was about 15 s. Spectra were analyzed with OPUS software.

Photopolymerization reactions were carried out in the reaction vessel where the reaction mixtures were irradiated by LED lights (red LED light, $\lambda_{\text{max}} = 635\text{ nm}$, 0.4 mW cm^{-2} ; blue LED light, $\lambda_{\text{max}} = 460\text{ nm}$, 0.7 mW cm^{-2}). LED lights and remote controller were purchased from RS Components Australia.

General procedure for the synthesis of *N*-acryloyl amino acid monomers

Synthesis of the monomers of *N*-acryloyl-DL-valine methyl ester (V-OMe), *N*-acryloyl-L-valine (LV), *N*-acryloyl-D-valine (DV), *N*-acryloyl-L-aspartic acid (LD), *N*-acryloyl-D-aspartic acid (DD), *N*-acryloyl-L-glutamic acid (LE), *N*-acryloyl-L-serine (LS) and *N*-acryloyl-D-phenylalanine (DF).

In a typical procedure (e.g. synthesis of the V-OMe) monomers were synthesized according to the literature²¹ using a modified procedure as follows; DL-valine methyl ester (2 g, 15.3 mmol) was dissolved in 10 mL of 1 M NaOH. Acryloyl chloride (1.66 g, 18.3 mmol) was added dropwise with stirring at 0 °C within 30 min. The pH of the solution was monitored using a pH meter and maintained at 10–11 by slow addition of 2 M NaOH. After adding acryloyl chloride, the reaction was kept at 0 °C for 30 min, and then warmed up to room temperature for another 4 h. After the solution was acidified to pH 2.0 by addition of 2 M HCl, the monomer was extracted with ethyl acetate (4 \times 40 mL), and the organic phase was dried with anhydrous sodium sulfate. After filtration and evaporation to remove most of the solvent, the concentrated solution was left standing overnight to crystallize. Colorless granular crystals were obtained with a yield above 80%.

Synthesis of *N*-acryloyl-L-Glu-OtBu (LE-OtBu)

L-Glu-OtBu (4 g, 15.0 mmol) and triethylamine (3.4 g, 34.0 mmol) was dissolved in 150 mL of DCM. Acryloyl chloride (1.67 g, 18.0 mmol) was added dropwise with stirring at 0 °C within 30 min. The reaction was kept at 0 °C for 30 min, and then at room temperature for another 4 h. The solution was washed by 1 M HCl (40 mL), saturated NaHCO₃ (40 mL), and saturated NaCl (40 mL), respectively. The organic phase was dried with anhydrous sodium sulfate. After filtration and

evaporation, the obtained monomer was purified by column chromatography using a silica gel (70–200 micron) packed column with DCM as the eluent. White powder was obtained with a yield above 80%.

General procedure for the synthesis of amino acid polymers by PET-RAFT polymerization

In typical procedure (e.g. polymerization of V-OMe) a reaction stock solution consisting of DMSO (0.65 mL), V-OMe (100 mg, 0.54 mmol), DTPA (1.26 mg, 0.0036 mmol) and Ir(ppy)₃ (0.0018 mg, 5 ppm relative to molar concentration of monomer) was prepared in a 4 mL glass vial. The glass vial was sealed with a rubber septum, and the reaction mixture was degassed with nitrogen for 20 minutes. The glass vial was irradiated under blue LED light strips ($\lambda_{\text{max}} = 460\text{ nm}$, 0.7 mW cm^{-2}) at room temperature. Monomer conversion was determined by ¹H NMR spectrum. The conversion was calculated by the integration of the monomer –C=C–H resonance at δ 5.6 ppm and comparison with the sum of the –CH–COOMe (α -H) peak intensities of polymer and monomer at δ 4.1 ppm. The resulting polymers (#6, Table 1) were purified by reprecipitation from MeOH in a large excess of diethyl ether. After three cycles of dissolution and precipitation, the polymers were dried under vacuum. The purified polymers were analyzed by UV-vis spectroscopy and ¹H NMR measurements to confirm chain end group fidelities and calculate absolute molecular weights, $M_{n, \text{NMR}}$.

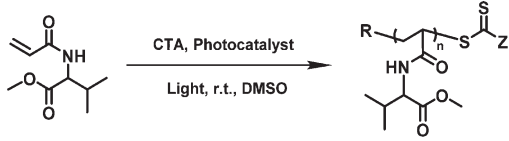
$$M_{n, \text{NMR}} = I^{4.1 \text{ ppm}} / (I^{1.2 \text{ ppm}} / 16) \times MW^{\text{V-OMe}} + MW^{\text{DTPA}}$$

where $I^{4.1 \text{ ppm}}$ and $I^{1.2 \text{ ppm}}$ correspond to integration of peak signals at δ 4.1 ppm and δ 1.2 ppm attributed to α -H (–CH–COOMe, 1H) of V-OMe and the alkyl chain end-group (16H) from DTPA.

General procedure for the kinetic study of PET-RAFT polymerization of *N*-acryloyl amino acid monomers

In a typical procedure (e.g. polymerization of V-OMe in DMSO) a reaction stock solution consisting of DMSO (0.6 mL), V-OMe (70 mg, 0.378 mmol), DTPA (1.3 mg, 0.0037 mmol), and Ir(ppy)₃ (0.0012 mg, 5 ppm relative to molar concentration of monomer) was dissolved in a 0.9 mL FTNIR quartz cuvette (1 cm \times 2 mm) and sealed with a rubber septum and covered with aluminum foil while degassing for 20 min with N₂. The cuvette was then irradiated under a blue LED light ($\lambda_{\text{max}} = 460\text{ nm}$, 0.7 mW cm^{-2}) at room temperature. Every 15 min, the solution was scanned by FTNIR measurements. The monomer conversions were calculated by the ratio of the integral of the wavenumber area 6220–6120 cm^{-1} at different time points to that at 0 min. Aliquots of the final reaction mixtures were analyzed by GPC to measure number average molecular weights ($M_{n, \text{GPC}}$), and dispersity (M_w/M_n).

The polymerization of the monomer LV in MeOH was investigated as follows: a reaction stock solution consisting of MeOH (1 mL), LV (150 mg, 0.876 mmol), DDMAT (2.1 mg, 0.0058 mmol), and Ir(ppy)₃ (0.0029 mg, 5 ppm relative to

Table 1 PET-RAFT polymerization of V-OMe under different reaction conditions^a


#	Photocatalyst (PC)	CTA	[M]/[CTA]/[PC]	[PC]/[M] (ppm)	Time (h)	<i>a</i> ^b (%)	<i>M</i> _{n, GPC} ^c (g mol ⁻¹)	<i>M</i> _w / <i>M</i> _n
1	Ir(ppy) ₃	DDMAT	150 : 1 : 7.5 × 10 ⁻⁴	5	2	84	17 270	1.16
2	ZnTPP	DDMAT	150 : 1 : 7.5 × 10 ⁻³	50	3	88	17 070	1.15
3	Eosin Y	DDMAT	150 : 1 : 7.5 × 10 ⁻³	50	3	70	14 530	1.18
4	Ir(ppy) ₃	DTPA	150 : 1 : 7.5 × 10 ⁻⁴	5	2	89	19 940	1.15
5	Ir(ppy) ₃	DTPA	100 : 1 : 5.0 × 10 ⁻⁴	5	2	81	12 620	1.17
6	Ir(ppy) ₃	DTPA	50 : 1 : 2.5 × 10 ⁻⁴	5	2	85	7040	1.14

^a Reactions were performed at room temperature under blue LED light ($\lambda_{\max} = 460$ nm, 0.7 mW cm⁻²) for Ir(ppy)₃ and Eosin Y, or red LED light ($\lambda_{\max} = 635$ nm, 0.4 mW cm⁻²) for ZnTPP in DMSO. ^b Monomer conversion determined by ¹H NMR spectroscopy. ^c Molecular weight and dispersity determined by GPC analysis (DMAc used as eluent) using PMMA standard for calibration.

molar concentration of monomer) was charged in a 4 mL glass vial and sealed with a rubber septum and covered with aluminum foil while degassing in an ice bath for 20 min with N₂. The vial was then irradiated under a blue LED light ($\lambda_{\max} = 460$ nm, 0.7 mW cm⁻²) at room temperature. Every 1 h, aliquots of the reaction mixtures were withdrawn and analyzed by ¹H NMR to measure the monomer conversions and GPC to measure number average molecular weights (*M*_{n, GPC}) and dispersity (*M*_w/*M*_n). Polymers with free carboxylic acid functionality were methylated by TMSCHN₂ prior to GPC measurement. For the methylation of polymer, about 20 μ L of reaction solution was mixed with 0.5 mL of MeOH and 1 mL of THF. After adding 0.1 mL of TMSCHN₂, the solution was stirred at room temperature for 4 h. After removing the solvent under nitrogen, the solid polymer was analyzed by GPC. The final number average molecular weight (*M*_{n, GPC}) of the original polymer before methylation was calibrated by the following formula:

$$M_{n, \text{GPC}} = (M_{n, \text{GPC}}^{\text{expt}} - MW^{\text{CTA}}) / (MW^{\text{M}} + 14) \times MW^{\text{M}} + MW^{\text{CTA}}$$

where *M*_{n, GPC}^{expt}, MW^{CTA} and MW^M correspond to the experimental molecular weight of the methylated polymer from GPC analysis, molar mass of CTA and molar mass of monomer, respectively.

When the polymerization was conducted in MeOH using Ir(ppy)₃ as photocatalyst, Ir(ppy)₃ was first dissolved in DMSO (1 mg mL⁻¹) and then added in MeOH due to the low solubility of Ir(ppy)₃ in MeOH. The added amount of Ir(ppy)₃ was determined according to the molar ratio of [photocatalyst]/[monomer].

General procedure for preparation of diblock copolymers by PET-RAFT polymerization

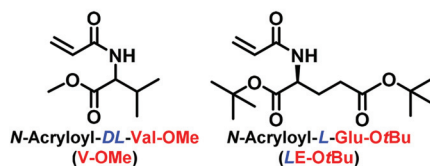
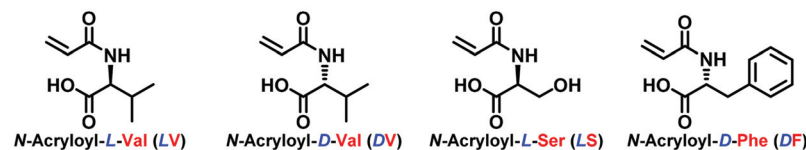
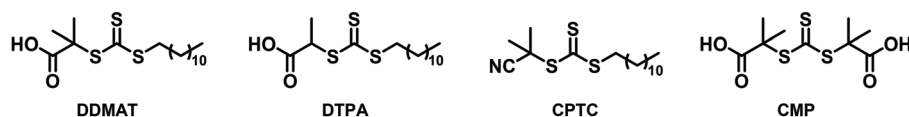
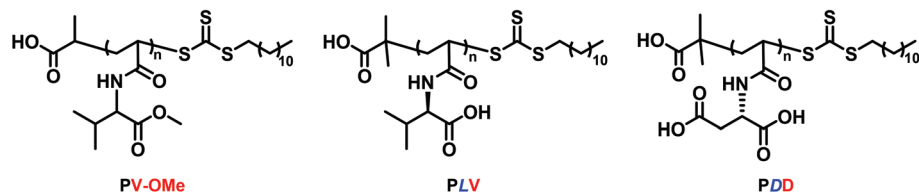
In a typical experiment (e.g. synthesis of the diblock copolymer poly(V-OMe)-*b*-poly(α -D) (PV-OMe-*b*-P α D)), a 4 mL glass vial was equipped with a rubber septum and charged with DMSO/MeOH (0.5 mL/0.5 mL), PV-OMe (20 mg, 0.0028 mmol), α D (77.5 mg, 0.027 mmol) and Ir(ppy)₃ (1.77 × 10⁻⁴ mg, 10 ppm

relative to molar concentration of monomer). After degassing with nitrogen for 20 minutes, the glass vial was irradiated under blue LED light ($\lambda_{\max} = 460$ nm, 0.7 mW cm⁻²) at room temperature. NMR and GPC analysis was performed as outlined above.

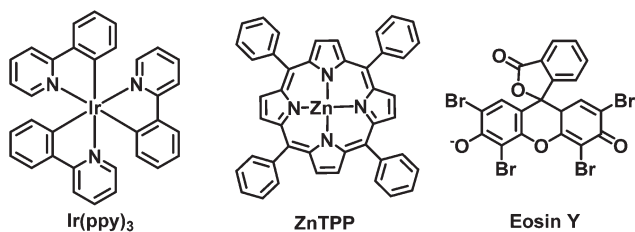
Results and discussion

PET-RAFT polymerization of *N*-acryloyl amino acid ester monomer

Considering the difficulty in synthesizing well-defined polymers with carboxylic acid functionality, the polymerization of the methylated monomer, *N*-acryloyl-DL-Val-OMe (V-OMe, Scheme 1), was first investigated using the PET-RAFT polymerization technique. V-OMe monomer was prepared by an amidation reaction between valine methyl ester and acryloyl chloride, and verified by ¹H and ¹³C NMR (ESI, Fig. S1 and S2[†]). Initially, the polymerization of V-OMe was performed in DMSO using Ir(ppy)₃ (Scheme 3) as photocatalyst, DDMAT (Scheme 2) as chain transfer agent (CTA) at the molar ratio of [V-OMe]/[CTA]/[photocatalyst] = 150 : 1 : 7.5 × 10⁻⁴ under blue light ($\lambda_{\max} = 460$ nm). A monomer conversion of 84% (determined by ¹H NMR) was obtained after 2 h of blue light irradiation. The obtained polymer, poly(*N*-acryloyl-DL-Val-OMe) (PV-OMe), displayed a low dispersity (*M*_w/*M*_n = 1.16, #1 in Table 1), although the molecular weight (*M*_{n, GPC} = 17 270 g mol⁻¹) was lower than theoretically predicted (*M*_{n, th} = 23 560 g mol⁻¹), likely due to the polymethyl methacrylate (PMMA) standards used for GPC calibration. ZnTPP and Eosin Y (Scheme 3) were also employed as photocatalysts for PET-RAFT polymerization of V-OMe (#2 and #3, Table 1). The resulting polymers showed well-controlled molecular weights and dispersities (*M*_w/*M*_n < 1.18). However, a higher catalyst loading (50 ppm *versus* 5 ppm) and longer reaction times (3 h *versus* 2 h) were required for ZnTPP and Eosin Y to achieve comparable monomer conversions when compared to Ir(ppy)₃ as photocatalyst, which is

N-acryloyl amino acid ester monomer**N-acryloyl amino acid monomers with mono-carboxylic acid functionality****N-acryloyl amino acid monomers with di-carboxylic acid functionality**Scheme 1 Chemical structure of *N*-acryloyl amino acid monomers investigated in this study.**RAFT Agent****Macro-RAFT Agent**

Scheme 2 Chemical structure of RAFT and macro-RAFT chain transfer agents (CTAs) employed in this study.



Scheme 3 Chemical structure of photocatalysts employed in this study.

consistent with our previous studies.^{45,56} All three photocatalysts have previously demonstrated the ability to be efficient and compatible for the PET-RAFT polymerization of most of

acrylates and acrylamides, and have also shown to be compatible for the amino acid monomers polymerized here.^{44,45,56}

When the polymerization of V-OMe was conducted using DTPA (Scheme 2) instead of DDMAT as the CTA, similar conversion and dispersity was obtained under identical conditions (#4, Table 1), suggesting the varied R groups on the two trithiocarbonates (DDMAT and DTPA) did not make any difference in polymerization control. According to the mechanism of PET-RAFT polymerization, these two trithiocarbonates could be easily activated to generate carbon radicals by Ir(ppy)₃ under blue light irradiation, and subsequently initiate and mediate polymerization efficiently. Other commonly used trithiocarbonates with different R groups, CPTC (Scheme 2) for instance, are also excellent CTAs for mediating the polymerization of *N*-acryloyl amino acid monomers. Subsequently,

different ratios of $[V\text{-OMe}]_0/[DTPA]_0 = 100/1$ or $50/1$ were investigated using PET-RAFT polymerization (#5 and #6 in Table 1). Low dispersities ($M_w/M_n < 1.20$) suggested a robust process for the polymerization of V-OMe using PET-RAFT technique.

^1H NMR spectrum of the purified PV-OMe (#6, Table 1) measured in $\text{DMSO-}d_6$ indicated that the peaks corresponding to polymer structure were clearly assigned (ESI, Fig. S3†). The M_n of PV-OMe was calculated by the integration of the peaks of polymer end group (dodecyl) at δ 1.2–1.3 ppm (16H) and that of $\alpha\text{-H}$ in the repeating monomer units at δ 3.9–4.5 ppm. The M_n of PV-OMe calculated by ^1H NMR spectrum ($M_{n, \text{NMR}} = 8610 \text{ g mol}^{-1}$) was in a good agreement with the theoretical value ($M_{n, \text{th}} = 8220 \text{ g mol}^{-1}$). However, the experimental molecular weight measured by GPC ($M_{n, \text{GPC}} = 7040 \text{ g mol}^{-1}$) was lower than $M_{n, \text{NMR}}$ and $M_{n, \text{th}}$, which is attributed to the PMMA standards used for calibration. UV-vis spectroscopy of PV-OMe after purification confirmed the presence of trithiocarbonate by the signal at the maximum of 305 nm (ESI, Fig. S4†). These preliminary results suggested that PET-RAFT polymerization is a facile and robust technique for synthesizing well-defined functional amino acid-based polymers.

In order to confirm the living radical process, the kinetics of PET-RAFT polymerization of V-OMe was investigated *via* online FTNIR measurement. The polymerization was carried out in a cuvette using DTPA as the RAFT agent and $\text{Ir}(\text{ppy})_3$ as photocatalyst under blue light irradiation ($\lambda_{\text{max}} = 460 \text{ nm}$, 0.7 mW cm^{-2}), at a molar ratio of $[V\text{-OMe}]/[DTPA]/[\text{Ir}(\text{ppy})_3] = 100 : 1 : 5 \times 10^{-4}$ in DMSO. Under blue light irradiation, the monomer conversions increased with light exposure time (Fig. 1A). By switching the light source “on” and “off”, the

polymerization was able to be reversibly activated and deactivated. Monomer consumption was only observed while light is “on”, suggesting the photocontrol of the polymerization (Fig. 1A and B). The induction period of the polymerization of V-OMe was 9 min, which is common in PET-RAFT polymerization and could originate from small amounts of residual oxygen or other trace impurities.^{45,50,57} The good agreement between the experimental and theoretical number-average molecular weights (M_n and $M_{n, \text{th}}$) as well as the linear increase in M_n versus monomer conversion, low dispersity (Fig. 1C), and symmetrical molecular weight distribution (Fig. 1D) further verified the living features of the process. Therefore, a well-controlled polymerization process of *N*-acryloyl amino acid ester monomer was confirmed.

PET-RAFT polymerization of *N*-acryloyl amino acid monomers with mono-carboxylic acid functionality

In this section, we investigated PET-RAFT polymerizations of the unprotected monomers with mono-carboxylic acid functionality. Carboxylic acid groups in amino acid-based polymers can interact with various metal ions, nonionic proton-accepting polymers, and cationic polyelectrolytes.^{6,39} As such, amino acid-based polymers with carboxylic acid groups are promising for producing tailored functional polymers for various applications. The unprotected monomer, *N*-acryloyl-L-Val (LV, Scheme 1, ^1H and ^{13}C NMR spectra shown in ESI, Fig. S5 and S6†) was first chosen to compare with the methylated monomer, V-OMe. DMSO has been demonstrated to be a good solvent for traditional PET-RAFT polymerization and V-OMe polymerization (*vide supra*) and was initially employed for the

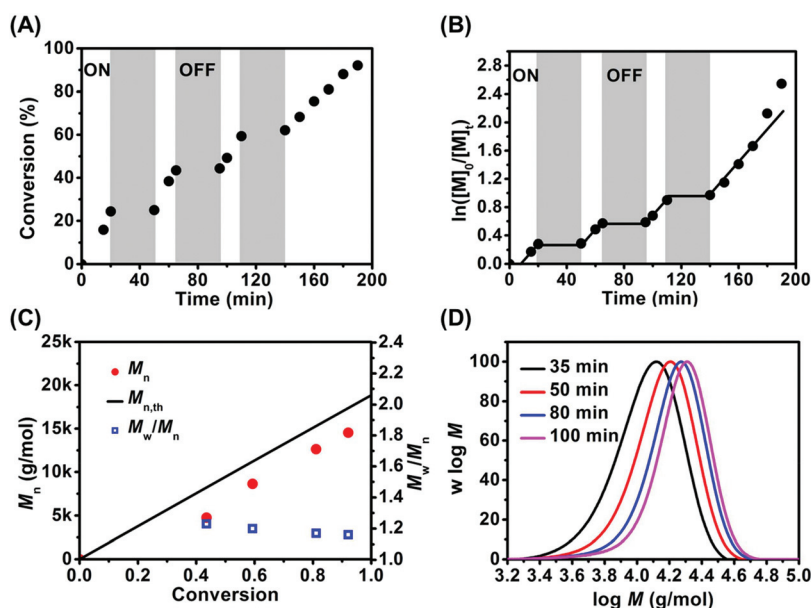


Fig. 1 Kinetic study of the PET-RAFT polymerization of V-OMe with DTPA as the CTA and $\text{Ir}(\text{ppy})_3$ as photocatalyst under blue light irradiation ($\lambda_{\text{max}} = 460 \text{ nm}$, 0.7 mW cm^{-2}), using a molar ratio of $[V\text{-OMe}]/[DTPA]/[\text{Ir}(\text{ppy})_3] = 100 : 1 : 5 \times 10^{-4}$ in DMSO. Dependence of (A) monomer conversion and (B) $\ln([M]_0/[M]_t)$ on the reaction time under blue light irradiation that was switched “on” and “off”. (C) $M_{n, \text{GPC}}$ and M_w/M_n versus monomer conversion. (D) Molecular weight distributions at different polymerization time intervals. Molecular weight and dispersity determined by GPC analysis (DMAc used as eluent) using PMMA standards for calibration.

polymerization of unprotected amino acid-based monomers. Ir(ppy)₃ was employed as photocatalyst due to its strong tolerance towards carboxylic acid functionality and widely used in visible light catalyzed organic transformation^{58,59} and photopolymerization.^{60,61} As shown in Table 2 (#1 and #2), the polymerizations of *l*V using either DDMAT or DTPA as CTA were not well controlled with dispersity close to 1.30 for both polymers, which was greater than that of PV-OMe ($M_w/M_n < 1.20$). Similarly, the other conventional solvents, including DMF, THF and Diox were even worse for polymerization control than DMSO, with dispersities >1.35 (ESI, Table S1†). Previous studies revealed that alcohols, such as MeOH and MeOH/toluene mixtures, were effective solvents for the controlled radical polymerization, particularly thermally induced RAFT polymerization, of *N*-acryloyl amino acid monomers with low dispersities.^{38,39} Therefore, we employed MeOH in our system to polymerize the same monomer under identical reaction conditions (#3, Table 2). Accordingly, the resulting polymer, poly(*N*-acryloyl-*L*-Val) (P*l*V), presented much lower dispersity ($M_w/M_n = 1.16$) and more uniform and symmetrical GPC curves (ESI, Fig. S7†), compared to those attained in DMSO. The solvent effect is most likely associated with the intrinsic strength of hydrogen bonding between monomer and polymer, or polymer and polymer, through the acid/acid or acid/amide functionalities in different solvents.^{62–64} Compared to MeOH, the stronger hydrogen bonding in DMSO makes the chain transfer less efficient; increased steric hindrance and constrained access of chain end radical species to the thiocarbonylthio chain ends leads to polymers with higher dispersities in DMSO. MeOH effectively prevents hydrogen bonding between both monomer and polymer, and polymer and polymer, which increases the efficiency of chain transfer and lowers polymer dispersities as a result.

After purification by precipitation, P*l*V was submitted for ¹H NMR analysis to confirm the chemical structure of the polymer (ESI, Fig. S8†). The trithiocarbonate end group of P*l*V

has a characteristic absorption at the maximum of 305 nm in UV-vis spectrum (ESI, Fig. S9†). Different molar ratios of $[M]_0/[CTA]_0 = 100/1$ and $50/1$ were also investigated for the polymerization of *l*V, indicating good control over molecular weights and low dispersities (#4 and #5, Table 2). In addition, poly(*N*-acryloyl-*D*-Val) (P*D*V) with *D*-configuration was also synthesized. Comparing the results of *l*V (#3, Table 2, 85%, $M_w/M_n = 1.16$) and *D*V (#6, Table 2, 83%, $M_w/M_n = 1.19$) under the same conditions, monomer chirality did not appear to affect the controlled polymerization process.

The polymerization kinetics of the PET-RAFT polymerization of *l*V was investigated in a glass vial using DDMAT as RAFT agent and Ir(ppy)₃ as photocatalyst, at a molar ratio of $[lV]/[DDMAT]/[Ir(ppy)_3] = 150:1:7.5 \times 10^{-4}$ in MeOH. The samples were withdrawn at different irradiation time intervals for determination of monomer conversions by ¹H NMR, and molecular weights and dispersity by GPC. The polymerization proceeded smoothly, evidenced by the increase of monomer conversion with the time of blue light irradiation (Fig. 2A). The plot of $\ln([M]_0/[M]_t)$ increased linearly versus exposure time, indicating a controlled polymerization process (Fig. 2B). The plot of $M_{n, GPC}$ versus monomer conversion also displayed a linear relationship (Fig. 2C), although the molecular weights are lower than theoretical ones due to the PMMA standards used for GPC calibration. The dispersities gradually decreased with the increase of monomer conversion (Fig. 2C), with polymer samples showing a clear shift from low to high molecular weights during the polymerization (Fig. 2D). These results further confirmed the living feature of PET-RAFT polymerization of *l*V.

To demonstrate the versatility and robustness of PET-RAFT polymerization of *N*-acryloyl amino acid monomers with mono-carboxylic acid functionality, two other *N*-acryloyl amino acid monomers, *N*-acryloyl-*D*-Phe, with phenyl moiety (*D*F, Scheme 1, ¹H and ¹³C NMR spectra shown in ESI, Fig. S10 and S11†), and *N*-acryloyl-*L*-Ser, with hydroxyl functionality (*l*S, ¹H

Table 2 PET-RAFT polymerization of *N*-acryloyl amino acid monomers with mono-carboxylic acid functionality using Ir(ppy)₃ as photocatalyst under different reaction conditions^a

#	Monomer	Solvent	CTA	$[M]/[CTA]/[PC]$	$[I]/[M]$ (ppm)	Time (h)	a^b (%)	$M_{n, GPC}^c$ (g mol ⁻¹)	M_w/M_n
1	<i>l</i> V	DMSO	DDMAT	$150:1:7.5 \times 10^{-4}$	5	4	94	17 930	1.27
2	<i>l</i> V	DMSO	DTPA	$150:1:7.5 \times 10^{-4}$	5	4	92	18 050	1.29
3	<i>l</i> V	MeOH	DDMAT	$150:1:7.5 \times 10^{-4}$	5	4	85	15 880	1.16
4	<i>l</i> V	MeOH	DDMAT	$100:1:5 \times 10^{-4}$	5	4.5	69	8420	1.17
5	<i>l</i> V	MeOH	DDMAT	$50:1:2.5 \times 10^{-4}$	5	4	44	2020	1.16
6	<i>D</i> V	MeOH	DDMAT	$150:1:7.5 \times 10^{-4}$	5	4	83	17 440	1.19
7	<i>D</i> F	DMSO	DTPA	$150:1:7.5 \times 10^{-4}$	5	2	41	15 480	1.63
8	<i>D</i> F	DMSO	CPTC	$150:1:7.5 \times 10^{-4}$	5	4.5	46	15 430	1.53
9	<i>D</i> F	DMSO	DDMAT	$150:1:1.5 \times 10^{-3}$	10	4	83	23 680	1.49
10	<i>D</i> F	MeOH	DDMAT	$150:1:1.5 \times 10^{-3}$	10	4	65	16 720	1.20
11	<i>l</i> S	MeOH	DDMAT	$150:1:1.5 \times 10^{-3}$	10	4	50	11 310	1.17

^a The reactions were performed using Ir(ppy)₃ as catalyst under blue LED light irradiation ($\lambda_{max} = 460$ nm, 0.7 mW cm⁻²) at room temperature.

^b Monomer conversion determined by ¹H NMR spectroscopy. ^c Molecular weight and dispersity determined by GPC analysis (DMAC used as eluent) using PMMA standard for calibration. The resulting polymer was methylated by TMSCHN₂ prior to GPC analysis.

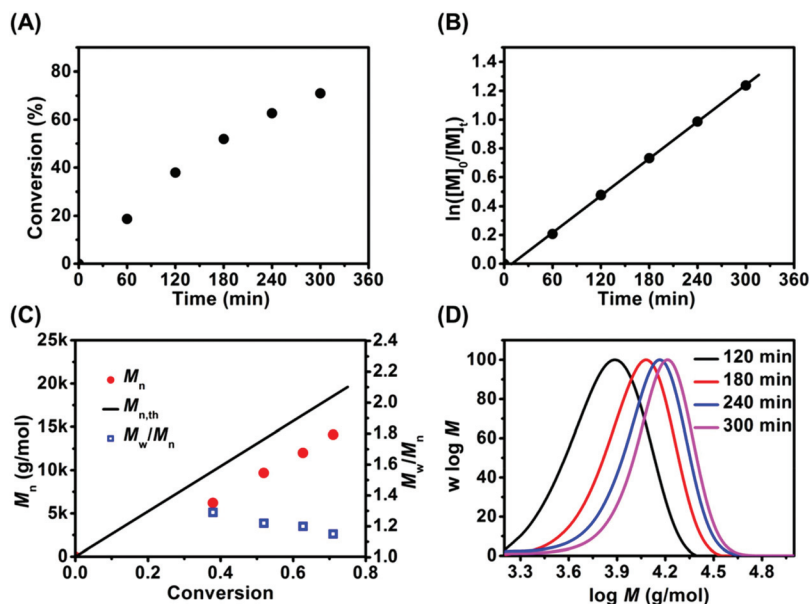


Fig. 2 Kinetics study of the PET-RAFT polymerization of LV with DDMAT as the CTA and Ir(ppy)₃ as photocatalyst under blue light irradiation ($\lambda_{\text{max}} = 460 \text{ nm}$, 0.7 mW cm^{-2}), using a molar ratio of [LV]/[DDMAT]/[Ir(ppy)₃] = 150 : 1 : 7.5×10^{-4} in MeOH. (A) Monomer conversion versus polymerization time. (B) $\ln([M]_0/[M]_t)$ versus polymerization time. (C) $M_{n, \text{GPC}}$ and M_w/M_n versus monomer conversion. (D) Molecular weight distributions at different polymerization time intervals. The resulting polymer was methylated by TMSCHN₂ prior to GPC analysis.

and ¹³C NMR spectra shown in ESI, Fig. S15 and S16†), were investigated. When DMSO was used as the solvent, the obtained poly(*N*-acryloyl-*D*-Phe) (P_DF) polymers showed broad dispersities ($M_w/M_n > 1.4$) regardless of RAFT agents (DTPA, CPTC and DDMAT) and catalyst loadings (5 and 10 ppm) (#7–#9, Table 2). However, similar to the polymerization of LV and DV, the polymerization of DF and LS in MeOH was successful and afforded P_DF with a low dispersity ($M_w/M_n = 1.20$, #10 in Table 2). The chemical structure of this resulting polymer and the presence of RAFT end-group were confirmed by ¹H NMR analysis (ESI, Fig. S12†) and UV-vis spectroscopy (ESI, Fig. S13†), respectively. The kinetic study of the polymerization of DF was also performed (ESI, Fig. S14†). The linear plot of $\ln([M]_0/[M]_t)$ against exposure time and $M_{n, \text{GPC}}$ against monomer conversion clearly indicated the living process of the DF polymerization. Previous studies revealed that thermally initiated RAFT polymerization of *N*-acryloyl-Phe can control the molecular weights and dispersities ($M_w/M_n > 1.22$), though the polymerization was carried out at elevated temperatures (>45 °C) and long reaction times (>24 h).³⁹ Compared with the thermally initiated RAFT polymerization at high temperature, the PET-RAFT technique is conducted at room temperature. This mild reaction conditions increases the selectivity of the radical reactions and minimizes unfavorable side reactions, such as accelerated radical transfer to solvents and impurities, gradual decomposition of RAFT agents.³⁹

In the case of LS polymerization, 50% of monomer conversion (determined by ¹H NMR) was obtained after 4 h of blue light irradiation. The $M_{n, \text{GPC}}$ of the poly(*N*-acryloyl-*L*-Ser) (P_LS, $M_{n, \text{GPC}} = 11\,310 \text{ g mol}^{-1}$) was consistent with the theoretical values ($M_{n, \text{th}} = 12\,300 \text{ g mol}^{-1}$), and the dispersity of the

polymer was low ($M_w/M_n = 1.17$, #11 in Table 2). The chemical structure of this resulting polymer was further confirmed by ¹H NMR analysis (ESI, Fig. S17†). As such, these results demonstrated that the PET-RAFT approach is versatile and robust for polymerization of *N*-acryloyl amino acid monomers with mono-carboxylic acid functionality.

PET-RAFT polymerization of *N*-acryloyl amino acid monomers with di-carboxylic acid functionality

PET-RAFT polymerization of *N*-acryloyl amino acid monomers with di-carboxylic acid functionality was investigated under various reaction conditions. The polymerization of *N*-acryloyl-*D*-Asp (P_DD, Scheme 1, ¹H and ¹³C NMR spectra shown in ESI, Fig. S18 and S19†) in different solvents, including DMSO and MeOH, was first studied. Similar trends on the dispersity were observed on switching solvents, where polymerizations performed in DMSO presented a high dispersity ($M_w/M_n = 1.45$, #1 in Table 3), whereas MeOH gave a low dispersity ($M_w/M_n = 1.13$, #2 in Table 3). The chemical structure of poly(*N*-acryloyl-*D*-Asp) (P_DD) was further confirmed by ¹H NMR analysis (ESI, Fig. S20†). UV-vis spectrum (ESI, Fig. S21†) of the polymer showed the typical UV absorption of the thiocarbonylthio group at the maximum of 305 nm. For comparison, thermally initiated RAFT polymerization of P_DD was investigated using 2,2'-azobisisobutyronitrile (AIBN) as initiator at 60 °C instead of Ir(ppy)₃ as photocatalyst at ambient temperature, under otherwise identical conditions (ESI, Table S2†). At a molar ratio of [P_DD]/[DDMAT]/[AIBN] = 150 : 1 : 1, the monomer conversion reached 93% after 8 h reaction and the dispersity of resultant P_DD homopolymer is higher than that in photo system ($M_w/M_n = 1.24$ (#1, ESI, Table S2†) vs. 1.13 (#2, Table 3)).

Table 3 PET-RAFT polymerization of *N*-acryloyl amino acid monomers with di-carboxylic acid functionality in different reaction conditions^a

#	Monomer	PC	Solvent	CTA	[M]/[CTA]/[PC]	[I]/[M] (ppm)	Time (h)	<i>a</i> ^b (%)	<i>M</i> _{n, GPC} ^c (g mol ⁻¹)	<i>M</i> _w / <i>M</i> _n
1	ⓁD	Ir(ppy) ₃	DMSO	DDMAT	150 : 1 : 1.5 × 10 ⁻³	10	6	96	27 180	1.45
2	ⓁD	Ir(ppy) ₃	MeOH	DDMAT	150 : 1 : 1.5 × 10 ⁻³	10	4	80	18 530	3
3	ⓁD	Eosin Y	MeOH	DDMAT	150 : 1 : 7.5 × 10 ⁻³	50	16	77	17 870	1.11
4	ⓁD	Eosin Y	H ₂ O	CMP	150 : 1 : 7.5 × 10 ⁻³	50	5	75	16 600	1.37
5	ⓁE	Ir(ppy) ₃	MeOH	DDMAT	100 : 1 : 1.0 × 10 ⁻³	10	6	70	13 060	1.13
6	ⓁE- <i>O</i> <i>t</i> Bu	Ir(ppy) ₃	DMSO	DDMAT	150 : 1 : 1.5 × 10 ⁻³	10	2	85	40 320	1.36
7	ⓁE- <i>O</i> <i>t</i> Bu	Ir(ppy) ₃	DMSO/MeCN ^d	DDMAT	150 : 1 : 1.5 × 10 ⁻³	10	3	50	16 500	1.20

^aThe reactions were performed under blue LED light irradiation ($\lambda_{\max} = 460 \text{ nm}$, 0.7 mW cm^{-2}) at room temperature. ^b Monomer conversion determined by ¹H NMR spectroscopy. ^c Molecular weight and dispersity were determined by GPC analysis (DMAc used as eluent) using PMMA standard for calibration. ^d The mixed solvent of DMSO/MeCN (1/1, v/v) was used to improve the solubility of the resultant polymer. The resulting polymers with carboxylic acid functionalities were methylated by TMSCHN₂ prior to GPC analysis.

Although lower AIBN concentration (molar ratio of [ⓁD]/[DDMAT]/[AIBN] = 150 : 1 : 0.5) was able to slightly improve the dispersity ($M_w/M_n = 1.20$), much longer polymerization time had been traded off (16 h for 88% monomer conversion). Therefore, the PET-RAFT process presented to be more advantageous for ⓁD polymerization than thermally initiated RAFT technique. However, it is not conclusive that PET-RAFT gives better control than conventional thermal RAFT because it will depend on case by case.

A kinetic study of the PET-RAFT polymerization of ⓁD in MeOH was investigated *via* ¹H NMR and GPC measurements. The monomer conversions continuously increased with blue light irradiation (Fig. 3A). The linear plot of $\ln([M]_0/[M]_t)$ versus exposure time (Fig. 3B) indicated that constant concentrations of propagating radicals were present during the

polymerization period, and almost no induction period was observed. The evolution of experimental *M*_n with monomer conversion showed a linear plot in excellent agreement with theoretical molecular weights (Fig. 3C). Monomodal molecular weight distributions with clear and complete shifts on increasing polymerization time were also observed (Fig. 3D), and low dispersity values revealed a good control of the polymerization.

To demonstrate the versatility of this polymerization technique, another photocatalyst, the organo-dye Eosin Y (Scheme 3), was investigated due to its non-toxicity and good solubility in many common solvents. The catalytic efficiency of Eosin Y was generally lower than that of Ir(ppy)₃, necessitating 16 h light irradiation and 50 ppm catalyst dosage, though the polymerizations catalyzed by Eosin Y produced polymers with

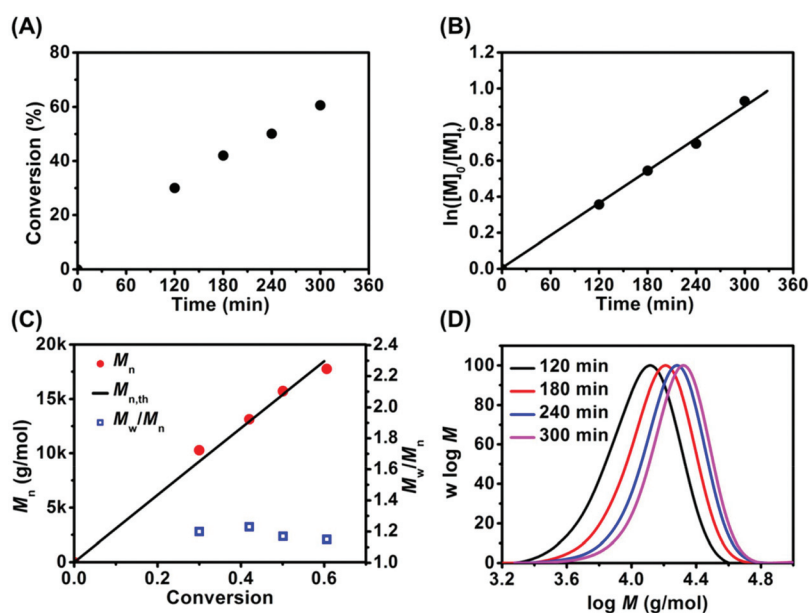


Fig. 3 Kinetic study of the PET-RAFT polymerization of ⓁD with DDMAT as the CTA and Ir(ppy)₃ as catalyst under blue light irradiation ($\lambda_{\max} = 460 \text{ nm}$, 0.7 mW cm^{-2}), using a molar ratio of [ⓁD]/[DDMAT]/[Ir(ppy)₃] = 150 : 1 : 1.5 × 10⁻³ in MeOH. (A) Monomer conversion versus polymerization time. (B) $\ln([M]_0/[M]_t)$ versus polymerization time. (C) *M*_{n, GPC} and *M*_w/*M*_n versus monomer conversion. (D) Molecular weight distributions at different polymerization time intervals. The resulting polymer was methylated by TMSCHN₂ before GPC analysis.

relatively low dispersities ($M_w/M_n = 1.11$, #3 in Table 3). Aqueous PET-RAFT polymerization of P_DD was also investigated using Eosin Y as photocatalyst, and CMP as aqueous RAFT agent (Scheme 2). In order to increase the solubility of CMP, the pH of the reaction solution was adjusted to 6.0 by addition of 1 M NaOH. 75% monomer conversion (determined by ¹H NMR) was obtained after 5 h light irradiation; however, a relatively high dispersity ($M_w/M_n = 1.37$, #4 in Table 3) was observed, which may be indicative that pH may impact the control of the polymerization. The polymerizations of monomers with carboxylic group were usually performed at natural pH (pK_a or isoelectric point).^{42,43,65,66} Lansalot and D'Agosto previously reported the RAFT polymerization of methacrylic acid (MAA) in water, where the polymerization lost the control when the solution pH was higher than the pK_a (4.36) of MAA.^{65,66} Under the condition of high pH, the hindrance effect induced by the electrostatic repulsion of fully ionized carboxylic acid groups caused a low k_p and deteriorated the addition-fragmentation steps in the RAFT process.⁶⁵ In our current system, the relatively high dispersity ($M_w/M_n = 1.37$) could be attributed to this effect.

Subsequently, *N*-acryloyl-L-Glu (LE, Scheme 1, ¹H and ¹³C NMR spectra shown in ESI, Fig. S22 and S23†), another monomer with di-carboxylic acid functionality, was investigated in MeOH. 70% monomer conversion of LE (#5, Table 3) was achieved after 6 h of irradiation. The corresponding polymer was obtained with an expected molecular weight ($M_n = 13\,060\text{ g mol}^{-1}$, #5 in Table 3) and low dispersity ($M_w/M_n = 1.13$). The chemical structure of poly(*N*-acryloyl-L-Glu) (PLE) was further confirmed by ¹H NMR analysis (ESI, Fig. S24†).

Previous studies have shown that protection of reactive functional groups (-NH₂, -COOH) is favorable for synthesizing well-defined polymers with side-chain amino acid monomers.^{2,3,32} For comparison, *N*-acryloyl glutamic acid with di-*tert*-butyl dicarbonate (*t*Bu) protection of carboxylic acid groups, was also investigated. *N*-Acryloyl-L-Glu-*Ot*Bu (LE-*Ot*Bu, Scheme 1) was synthesized by an amidation reaction; the chemical structure was verified by ¹H and ¹³C NMR spectra (ESI, Fig. S25 and S26†). LE-*Ot*Bu is soluble in MeCN, toluene, and DMSO, etc., while it is insoluble in alcohol and water.

When the polymerization was conducted in DMSO, 85% monomer conversion was achieved after 2 h irradiation; however, the corresponding poly(*N*-acryloyl-L-Glu-*Ot*Bu) (PLE-*Ot*Bu, Fig. S27 in ESI†) did not solubilize well resulting in precipitation of the polymers at high monomer conversions. Consequently, the resulting polymer exhibited a high dispersity ($M_w/M_n = 1.36$, #6 in Table 3). Although toluene and MeCN could improve polymer solubility, the polymerization conducted in either solvent presented negligible monomer conversion. In order to increase solubility while maintaining non-negligible polymerization rate, a mixed solvent system containing a mixture of DMSO/MeCN (1/1, v/v) was studied (#7, Table 3). Improved solubility of the prepared polymer led to better control over the molecular weight and dispersity ($M_w/M_n = 1.20$), however, the polymerization rate was much lower (50% monomer conversion after 3 h irradiation) compared to the pure DMSO system (85% monomer conversion after 2 h irradiation). As such, it appears that protecting reactive functional groups of the LE monomers may not be beneficial, because more stringent reaction conditions were required for effective polymerization.

Preparation of diblock copolymers of various *N*-acryloyl amino acid monomers

Successful chain extension of polymers formed in controlled/“living” radical polymerization is an important criterion for the confirmation of both integrity of the dormant end-group, and “living” character of the polymers. Thus, chain extensions of poly(*N*-acryloyl amino acid) polymers with various *N*-acryloyl amino acid monomers were performed. A PV-OMe macro-RAFT agent ($M_n = 7240\text{ g mol}^{-1}$, $M_w/M_n = 1.14$, Scheme 2) was synthesized by PET-RAFT polymerization and purified by precipitation. The synthesis of block copolymers of PV-OMe-*b*-P_DD was first conducted in MeOH; however, the obtained PV-OMe-*b*-P_DD exhibited a high dispersity ($M_w/M_n = 3.33$, #1 in Table 4). The GPC traces (#1 in Fig. 4) demonstrated that the chromatograms of PV-OMe-*b*-P_DD had a broad shoulder in the low molecular weight region, which represented the unreacted PV-OMe macro-RAFT agent; this was most likely caused by the poor solubility of PV-OMe macro-RAFT agent in MeOH. In

Table 4 PET-RAFT polymerization of diblock copolymers under different reaction conditions^a

#	Monomer	Solvent	CTA	Time (h)	a^b (%)	$M_{n,\text{GPC}}^c$ (g mol ⁻¹)	M_w/M_n
1	D _D	MeOH	PV-OMe ($M_n = 7240$, $M_w/M_n = 1.14$)	4	69	27 110	3.33
2	D _D	DMSO	PV-OMe ($M_n = 16\,760$, $M_w/M_n = 1.16$)	6	90	43 770	1.48
3 ^d	D _D	MeOH/DMSO	PV-OMe ($M_n = 7240$, $M_w/M_n = 1.14$)	4	57	23 050	1.34
4 ^d	D _D	MeOH/DMSO	PtV ($M_n = 13\,100$, $M_w/M_n = 1.15$)	8	60	28 120	1.29
5	D _D	MeOH	PtV ($M_n = 10\,860$, $M_w/M_n = 1.13$)	6	70	30 510	1.21
6	L _V	MeOH	PtV ($M_n = 10\,860$, $M_w/M_n = 1.13$)	6	82	31 920	1.14
7	L _D	MeOH	PtV ($M_n = 10\,860$, $M_w/M_n = 1.13$)	6	84	34 430	1.19
8	L _V	MeOH	P _D D ($M_n = 17\,870$, $M_w/M_n = 1.11$)	6	76	37 390	1.18

^a The reactions were performed at room temperature with Ir(ppy)₃ as catalyst under blue LED light irradiation ($\lambda_{\text{max}} = 460\text{ nm}$, 0.7 mW cm^{-2}) using $[M]/[CTA]/[\text{photocatalyst}] = 150 : 1 : 1.50 \times 10^{-3}$. ^b Monomer conversion determined by ¹H NMR spectroscopy. ^c Molecular weight and dispersity were determined by GPC analysis (DMAc used as eluent) using PMMA standard for calibration. ^d The ratio of MeOH/DMSO in the mixed solution was 1/1 (v/v). The resulting polymers were methylated by TMSCHN₂ prior to GPC measurement.

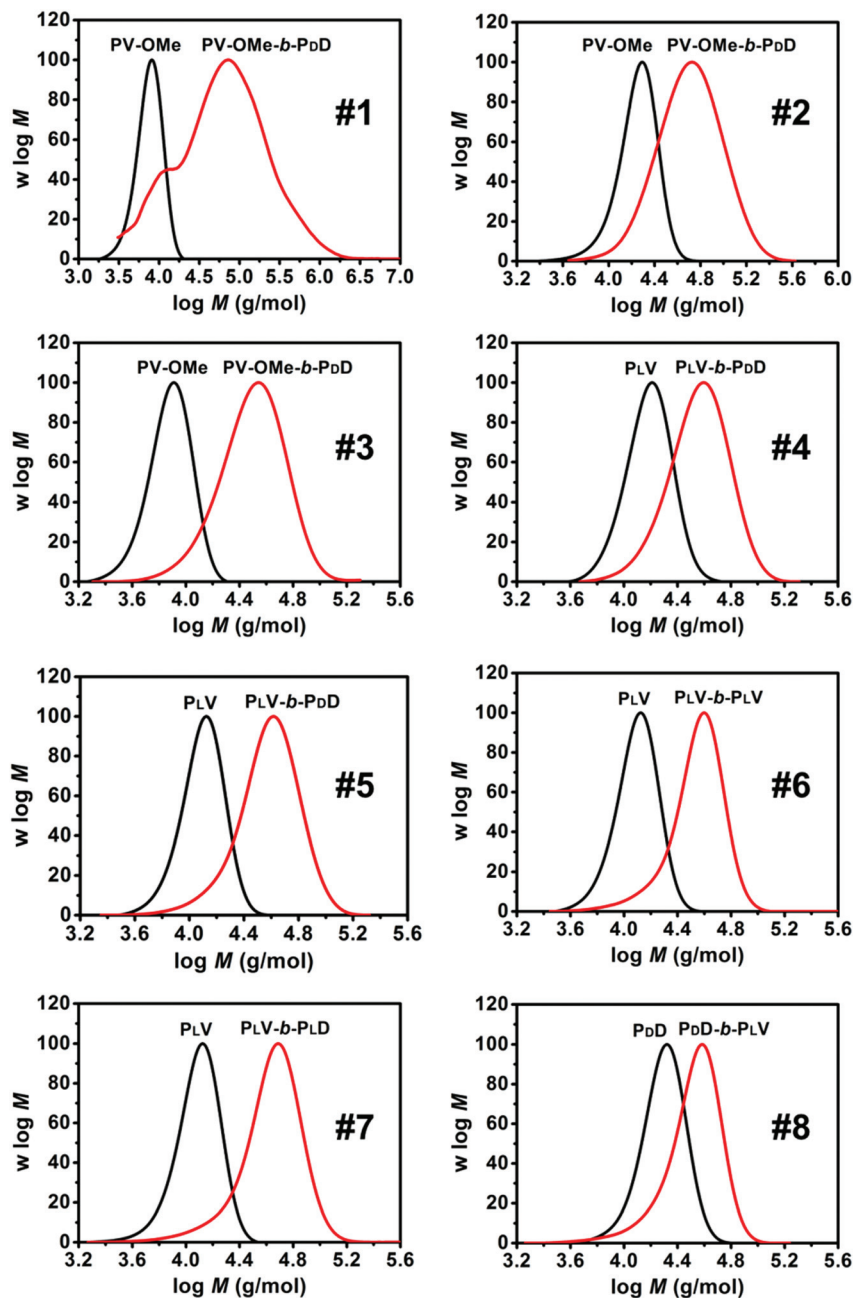


Fig. 4 GPC curves of the starting macro-RAFT agents and the diblock copolymers corresponding to Table 4. The resulting polymers with carboxylic acid functionalities were methylated by TMSCHN₂ prior to GPC measurement.

contrast, the polymerization conducted in DMSO improved the solubility of PV-OMe and afforded the diblock copolymer with lower dispersity ($M_w/M_n = 1.48$, #2, Table 4) with a reduced shoulder peak in molecular weight distribution (#2, Fig. 4). Since DMSO improved the solubility of the macro-RAFT agent, while MeOH improved control over the polymerization of *bD*, the polymerization of block copolymers was then conducted in the mixed solvent of MeOH/DMSO (1/1, v/v). As expected, well-defined diblock copolymers with relatively low dispersity ($M_w/M_n = 1.34$, #3 in Table 4 and Fig. 4) were obtained. ¹H NMR spectrum of PV-OMe-*b*-PdD in DMSO-*d*₆ clearly showed peaks

corresponding to both blocks (ESI, Fig. S28[†]). The end-group (trithiocarbonate) of PV-OMe-*b*-PdD was also confirmed by UV-vis spectroscopy (ESI, Fig. S29[†]).

PLV macro-RAFT agent ($M_n = 13\,100\text{ g mol}^{-1}$, $M_w/M_n = 1.15$, Scheme 2) with carboxylic acid functionalities was then investigated for chain extension. To compare with the results of PV-OMe macro-RAFT (#3, Table 4), the polymerization of *bD* using PLV as macro-RAFT agent (#4, Table 4) was first performed in mixed MeOH/DMSO (1/1, v/v) as solvent, at the same ratio of $[M]/[CTA]/[\text{photocatalyst}]$. Although the reaction time was required to be doubled (8 h) to achieve comparable

monomer conversion, the dispersity of the resulting P_LV-*b*-P_DD diblock copolymer was lower ($M_w/M_n = 1.29$, #4 in Table 4 and Fig. 4). Pure MeOH was then employed for polymerization under identical conditions (#5, Table 4), which resulted in an expected lower dispersity ($M_w/M_n = 1.21$). Owing to the favorable chain extension results in pure MeOH, P_LV macro-RAFT agent was subsequently chain extended with other chiral monomers, *L*V and *L*D, in MeOH (#6 and #7, Table 4). The diblock copolymers displayed low dispersities ($M_w/M_n = 1.14$ and 1.19, respectively for chain extension with *L*V and *L*D) and symmetrical GPC curves without any obvious tailing or shoulders (#6 and #7 in Fig. 4). Similarly, using P_DD as macro-RAFT agent ($M_n = 17\,870\text{ g mol}^{-1}$, $M_w/M_n = 1.11$, Scheme 2), P_DD-*b*-P_LV diblock copolymers with $M_n = 37\,390\text{ g mol}^{-1}$ and $M_w/M_n = 1.18$ were obtained after successful chain extension (#8 in Table 4 and Fig. 4). These results clearly demonstrate that chain extension of the macro-RAFT agent with various *N*-acryloyl amino acid monomers is possible, and can be robustly achieved to provide block copolymers with as-designed chain structures, regardless of the monomer chirality and block sequence.

Conclusion

In summary, a series of well-defined amino acid-based polymers with a variety of functional groups has been synthesized directly from the corresponding *N*-acryloyl amino acid monomers without protecting groups (carboxylic acid), using a photoinduced living radical process, namely photoinduced electron/energy transfer-reversible addition-fragmentation chain transfer (PET-RAFT). Controlled molecular weights and low dispersities ($M_w/M_n < 1.20$) were realized for homopolymers and diblock copolymers with diverse monomer chirality and block sequence. Various solvents and trithiocarbonate RAFT agents have shown to be effective for amino acid-based polymer preparation. Moreover, the three photocatalysts used in this study were effective for the PET-RAFT polymerization of amino acid-based monomers, and allow for reaction conditions to be tailored based on required physical and chemical properties, such as solubility, light absorption and stability. As such, the PET-RAFT process clearly provides a robust and versatile protocol for the precise synthesis of amino acid-based polymers. MeOH was certified to be an excellent solvent for the polymerization of *N*-acryloyl amino acid monomers with carboxylic acid functionality, regardless of the category of amino acid or the number of the carboxylic acid functionalities in the monomer structure. This contribution provides a library of amino acid-based polymers for the application of new materials design and macromolecular engineering.

Conflicts of interest

The authors declare no competing financial interest.

Acknowledgements

J. X. and C. B. acknowledges Australian Research Council (ARC) for their Future Fellowships (FT160100095 and FT120100096). X. W. thanks the National Natural Science Foundation (21574008) and the Fundamental Research Funds for the Central Universities (BHYC1705B and XK1701) of China for their financial support.

References

- 1 X. Q. Dou and C. L. Feng, *Adv. Mater.*, 2017, **29**, 1604062.
- 2 S. G. Roy and P. De, *J. Appl. Polym. Sci.*, 2014, **131**, 41084.
- 3 K. Bauri, S. G. Roy and P. De, *Macromol. Chem. Phys.*, 2016, **217**, 365–379.
- 4 E. R. Brisson, Z. Xiao and L. A. Connal, *Aust. J. Chem.*, 2016, **69**, 705–716.
- 5 H. Sun, F. Meng, A. A. Dias, M. Hendriks, J. Feijen and Z. Zhong, *Biomacromolecules*, 2011, **12**, 1937–1955.
- 6 H. Xu, Q. Yao, C. Cai, J. Gou, Y. Zhang, H. Zhong and X. Tang, *J. Controlled Release*, 2015, **199**, 84–97.
- 7 W. Wu, D. Xie, A. Puckett and J. W. Mays, *Eur. Polym. J.*, 2003, **39**, 959–968.
- 8 W. Xiong, X. Fu, Y. Wan, Y. Sun, Z. Li and H. Lu, *Polym. Chem.*, 2016, **7**, 6375–6382.
- 9 Y. Liu, X. Jin, X. Zhang, M. Han and S. Ji, *Carbohydr. Polym.*, 2015, **117**, 312–318.
- 10 Y. Wan, L. Liu, S. Yuan, J. Sun and Z. Li, *Langmuir*, 2017, **33**, 3234–3240.
- 11 R. E. Hancock and H. G. Sahl, *Nat. Biotechnol.*, 2006, **24**, 1551–1557.
- 12 A. Bogomolova, S. Keller, J. Klingler, M. Sedlak, D. Rak, A. Sturcova, M. Hruby, P. Stepanek and S. K. Filippov, *Langmuir*, 2014, **30**, 11307–11318.
- 13 Q. Liu, A. Singh and L. Liu, *Biomacromolecules*, 2012, **14**, 226–231.
- 14 Q. Liu, A. Singh and L. Liu, *Biomacromolecules*, 2013, **14**, 226–231.
- 15 X. Wang, H. Gan and T. Sun, *Adv. Funct. Mater.*, 2011, **21**, 3276–3281.
- 16 X. Wang, H. Gan, T. Sun, B. Su, H. Fuchs, D. Vestweber and S. Butz, *Soft Matter*, 2010, **6**, 3851–3855.
- 17 A. Lekchiri, J. Morcellet and M. Morcellet, *Macromolecules*, 1987, **20**, 49–53.
- 18 Y. Jin, F. Ye, C. Wu, Y.-H. Chan and D. T. Chiu, *Chem. Commun.*, 2012, **48**, 3161–3163.
- 19 B. S. Lokitz, A. J. Convertine, R. G. Ezell, A. Heidenreich, Y. Li and C. L. McCormick, *Macromolecules*, 2006, **39**, 8594–8602.
- 20 Y. Ni, J. Sun, Y. Wei, X. Fu, C. Zhu and Z. Li, *Biomacromolecules*, 2017, **18**, 3367–3374.
- 21 A. Bentolila, I. Vlodaysky, R. Ishai-Michaeli, O. Kovalchuk, C. Haloun and A. J. Domb, *J. Med. Chem.*, 2000, **43**, 2591–2600.

- 22 C. Deng, J. Wu, R. Cheng, F. Meng, H.-A. Klok and Z. Zhong, *Prog. Polym. Sci.*, 2014, **39**, 330–364.
- 23 Y. Shen, X. Fu, W. Fu and Z. Li, *Chem. Soc. Rev.*, 2015, **44**, 612–622.
- 24 H. Lu, J. Wang, Z. Song, L. Yin, Y. Zhang, H. Tang, C. Tu, Y. Lin and J. Cheng, *Chem. Commun.*, 2014, **50**, 139–155.
- 25 G. Gao, F. Sanda and T. Masuda, *Macromolecules*, 2003, **36**, 3932–3937.
- 26 R. Liu, F. Sanda and T. Masuda, *Macromolecules*, 2008, **41**, 5089–5097.
- 27 K. Bauri, S. G. Roy, S. Pant and P. De, *Langmuir*, 2013, **29**, 2764–2774.
- 28 J. Skey, C. F. Hansell and R. K. O'Reilly, *Macromolecules*, 2010, **43**, 1309–1318.
- 29 N. Higashi, D. Sekine and T. Koga, *J. Colloid Interface Sci.*, 2017, **500**, 341–348.
- 30 V. Ladmiraal, A. Charlot, M. Semsarilar and S. P. Armes, *Polym. Chem.*, 2015, **6**, 1805–1816.
- 31 R. K. O'Reilly, *Polym. Int.*, 2010, **59**, 568–573.
- 32 H. Mori and T. Endo, *Macromol. Rapid Commun.*, 2012, **33**, 1090–1107.
- 33 C. J. Hawker, A. W. Bosman and E. Harth, *Chem. Rev.*, 2001, **101**, 3661–3688.
- 34 I.-D. Chung, P. Britt, D. Xie, E. Harth and J. Mays, *Chem. Commun.*, 2005, 1046–1048.
- 35 K. Matyjaszewski, *Macromolecules*, 2012, **45**, 4015–4039.
- 36 C. Barner-Kowollik and S. Perrier, *J. Polym. Sci., Part A: Polym. Chem.*, 2008, **46**, 5715–5723.
- 37 A. B. Lowe and C. L. McCormick, *Prog. Polym. Sci.*, 2007, **32**, 283–351.
- 38 H. Mori, K. Sutoh and T. Endo, *Macromolecules*, 2005, **38**, 9055–9065.
- 39 M. M. Hideharu Mori, K. Sutoh and T. Endo, *Macromolecules*, 2006, **39**, 4351–4360.
- 40 A. Vaish, S. G. Roy and P. De, *Polymer*, 2015, **58**, 1–8.
- 41 S. Kumar, S. G. Roy and P. De, *Polym. Chem.*, 2012, **3**, 1239–1248.
- 42 B. S. Lokitz, A. W. York, J. E. Stempka, N. D. Treat, Y. Li, W. L. Jarrett and C. L. McCormick, *Macromolecules*, 2007, **40**, 6473–6480.
- 43 B. S. Lokitz, J. E. Stempka, A. W. York, Y. Li, H. K. Goel, G. R. Bishop and C. L. McCormick, *Aust. J. Chem.*, 2006, **59**, 749–754.
- 44 J. Xu, K. Jung, A. Atme, S. Shanmugam and C. Boyer, *J. Am. Chem. Soc.*, 2014, **136**, 5508–5519.
- 45 J. Xu, S. Shanmugam, H. T. Duong and C. Boyer, *Polym. Chem.*, 2015, **6**, 5615–5624.
- 46 J. Xu, S. Shanmugam, C. Fu, K.-F. Aguey-Zinsou and C. Boyer, *J. Am. Chem. Soc.*, 2016, **138**, 3094–3106.
- 47 J. Xu, C. Fu, S. Shanmugam, C. J. Hawker, G. Moad and C. Boyer, *Angew. Chem., Int. Ed.*, 2017, **56**, 8376–8383.
- 48 S. Shanmugam, J. Xu and C. Boyer, *Macromolecules*, 2014, **47**, 4930–4942.
- 49 J. Xu, K. Jung and C. Boyer, *Macromolecules*, 2014, **47**, 4217–4229.
- 50 Y. Chu, Z. Huang, K. Liang, J. Guo, C. Boyer and J. Xu, *Polym. Chem.*, 2018, **9**, 1666–1673.
- 51 S. Shanmugam, J. Xu and C. Boyer, *Angew. Chem., Int. Ed.*, 2016, **55**, 1036–1040.
- 52 S. Shanmugam, J. Xu and C. Boyer, *Macromolecules*, 2016, **49**, 9345–9357.
- 53 S. Shanmugam, J. Xu and C. Boyer, *Macromolecules*, 2017, **50**, 1832–1846.
- 54 J. T. Lai, D. Filla and R. Shea, *Macromolecules*, 2002, **35**, 6754–6756.
- 55 L. Couvreur, C. Lefay, J. Belleney, B. Charleux, O. Guerret and S. Magnet, *Macromolecules*, 2003, **36**, 8260–8267.
- 56 S. Shanmugam, J. Xu and C. Boyer, *J. Am. Chem. Soc.*, 2015, **137**, 9174–9185.
- 57 P. De, S. R. Gondi, D. Roy and B. S. Sumerlin, *Macromolecules*, 2009, **42**, 5614–5621.
- 58 Z. Zuo and D. W. C. MacMillan, *J. Am. Chem. Soc.*, 2014, **136**, 5257–5260.
- 59 G. Bergonzini, C. Cassani and C. J. Wallentin, *Angew. Chem., Int. Ed.*, 2015, **54**, 14066–14069.
- 60 B. P. Fors and C. J. Hawker, *Angew. Chem., Int. Ed.*, 2012, **51**, 8850–8853.
- 61 N. J. Treat, B. P. Fors, J. W. Kramer, M. Christianson, C.-Y. Chiu, J. Read de Alaniz and C. J. Hawker, *ACS Macro Lett.*, 2014, **3**, 580–584.
- 62 A. Chapiro, *Pure Appl. Chem.*, 1981, **53**, 643–655.
- 63 A. K. Mukherjee, K. S. Schmitz and L. B. Bhuiyan, *Langmuir*, 2004, **20**, 11802–11810.
- 64 H. Tanaka and T. Araki, *Phys. Rev. Lett.*, 2000, **85**, 1338–1341.
- 65 I. Chaduc, A. Crepet, O. Boyron, B. Charleux, F. D'Agosto and M. Lansalot, *Macromolecules*, 2013, **46**, 6013–6023.
- 66 I. Chaduc, M. Lansalot, F. D'Agosto and B. Charleux, *Macromolecules*, 2012, **45**, 1241–1247.